Advanced Composite Materials
Publication details, including instructions for authors and subscription information:
http://www.tandfonline.com/loi/tacm20

Dependence of Weibull parameters on the diameter and the internal defects of Tyranno ZMI fiber in the strength analysis

Tetsuya Morimoto [a], Koji Yamamoto [b] & Shinji Ogihara [c]

[a] Japan Aerospace Exploration Agency, 7-44-1 Jindaiji-higashi-machi, Chofu-shi, Tokyo 182-8522, Japan

[b] Department of Mechanical Engineering, Tokyo University of Science, 2641 Yamazaki, Noda, Chiba 278-8510, Japan

[c] Department of Mechanical Engineering, Tokyo University of Science, 2641 Yamazaki, Noda-shi, Chiba 278-8510, Japan

Version of record first published: 02 Apr 2012.

To cite this article: Tetsuya Morimoto, Koji Yamamoto & Shinji Ogihara (2007): Dependence of Weibull parameters on the diameter and the internal defects of Tyranno ZMI fiber in the strength analysis, Advanced Composite Materials, 16:3, 245-258

To link to this article: http://dx.doi.org/10.1163/156855107781393768

Adv. Composite Mater., Vol. 16, No. 3, pp. 245–258 (2007)

Also available online - www.brill.nl/acm

Dependence of Weibull parameters on the diameter and the internal defects of Tyranno ZMI fiber in the strength analysis

TETSUYA MORIMOTO [1,*], KOJI YAMAMOTO [2] and SHINJI OGIHARA [3]

[1] *Japan Aerospace Exploration Agency, 7-44-1 Jindaiji-higashi-machi, Chofu-shi, Tokyo 182-8522, Japan*
[2] *Department of Mechanical Engineering, Tokyo University of Science, 2641 Yamazaki, Noda, Chiba 278-8510, Japan (From April 1st, 2006: TOYOTA Industries Corp., 2-1 Toyota-cho, Kariya-shi Aichi 448-8671, Japan)*
[3] *Department of Mechanical Engineering, Tokyo University of Science, 2641 Yamazaki, Noda-shi, Chiba 278-8510, Japan*

Received 31 July 2006; accepted 10 November 2006

Abstract—The single-modal Weibull model has been assessed on Tyranno ZMI Si-Zr-C-O fiber if a set of shape and scale parameters accurately reproduced the effect of the size of the diameter on strength. The tensile data of a single fiber have been divided into two expedient groups as ‘small diameter’ group and ‘large diameter’ group in deriving the parameters, which should be consistent if the Weibull model accurately reproduced the size effect. However, the derived Weibull parameters were inconsistent between the two groups. Thereby the authors have concluded that the parameters of the single-modal Weibull model are dependent on the fiber diameter, so that the model is inadequate to reproduce the strength size effect. On the other hand, Weibull parameters were found consistent between the two groups by excluding the data of ‘large mirror zone’ sample, which was defined as the sample around 10% mirror zone area of the fracture surface. What is more, the exclusion reduced the strength variance more drastically in the ‘large diameter’ group than in the ‘small diameter’ group, even though the ‘large mirror zone’ samples were found identical in the percentage between the two groups. The authors therefore conclude that diameter limitation to the ‘small diameter’ group level can lead to drastically less distributed strength values than the estimated strength through the Weibull scaling on the present Tyranno ZMI Si-Zr-C-O fiber.

Keywords: Weibull model; size effect; Tyranno ZMI Si-Zr-C-O fiber; fiber diameter; SEM fractograph; tensile strength.

Edited by the JSCM.

*To whom correspondence should be addressed. E-mail: morimoto@chofu.jaxa.jp

1. INTRODUCTION

Drastic improvement is required for structural materials if they are to be utilized for applications in extreme conditions, such as those met with in reusable launch vehicles, automotive gas turbines and fusion power systems. Metallic materials possess a limited potential, so advanced composite materials, such as ceramic matrix composites (CMCs) and carbon/carbon composites (C/Cs), are under intensive study [1–5].

Brittle fibers, such as those used for the reinforcement of CMCs and C/Cs, have been known to reduce the tensile strength by increasing the gauge length. The 'size effect' is often reproduced with single-modal Weibull strength scaling [6, 7]; however, bias has been reported on some fibers [8, 9] and variable diameter has been focused on as one of the factors [10–13]. The bias negates the composite design and operational standards that are based on Weibull scaling. Thus, full understanding is required for the bias factors to ensure the composite component reliability.

Tyranno ZMI Si-Zr-C-O amorphous fiber (UBE Industry Co.) is a promising reinforcement for CMCs due to the excellence of its resistance to heat and oxidation [14]. It has been reported however that Tyranno ZMI fiber shows variable diameter, both at a bundle cross-section and along each gauge [15, 16]. The large diameter portion may contain miscrystallized phase in the amorphous phase. In addition, the diameter and the contaminant particle density may show some systematic relationship as the particles can affect the fiber spinning process. In such cases, the parameters of a single-modal Weibull model can behave as if they were the functions of fiber diameter and lead to a large bias of an estimated tensile strength from an experimental result. We have thus assessed in this study if the type and the density of fiber fracture sources are variable with diameter. Firstly, tensile tests have been conducted on several diameter samples to assess if the Weibull parameters were variable with diameter. Secondly, the fracture surfaces have been analyzed with a scanning electron microscope (SEM) to detect the dominant factors of the strength bias, and then the results were correlated with the fiber diameter. A possible improvement has then been discussed with regard to the dispersion and the mean of the tensile strength.

2. EXPERIMENTAL PROCEDURE

2.1. Sample preparation

The mechanical properties and chemical composition of Tyranno ZMI Si-Zr-C-O fiber, as reported by the supplier, UBE Industry Co., are given in Table 1 [17].

It has been reported that the variation in diameter of Tyranno ZMI is not negligible, either in bundle cross-section or along each gauge, with regard to its effect on the strength [16]. In this work, too, SEM analyses have revealed that the cross-section diameter of a bundle is widely variable, as shown in Fig. 1. Thus, to avoid the bias due to the diameter variability, whole gauge measurements have

Table 1.
Mechanical properties and chemical compositions of Tyranno ZMI fiber

Fiber diameter (μm)		11
Tensile strength (GPa)		3.4
Tensile modulus (GPa)		200
Elongation (%)		1.7
Chemical compositions (wt%)	Si	56.6
	C	34.8
	O	7.6
	Zr	1

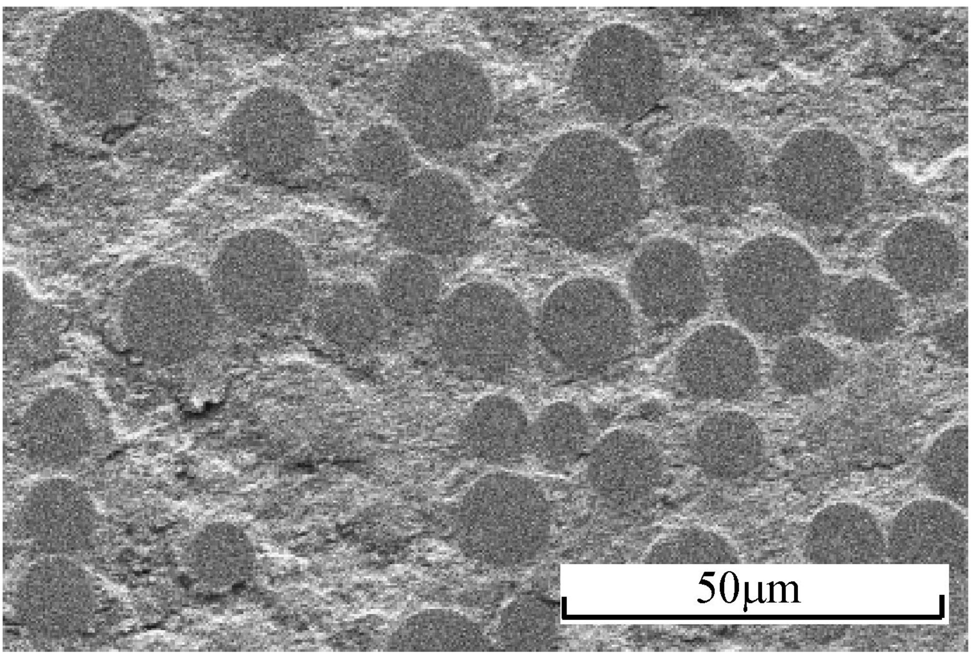

Figure 1. Cross-sections of Tyranno ZMI fibers.

been conducted with a laser scan micrometer LSM-500 (Mitutoyo Corp.) to collect uniform diameter portions as the tensile test samples. The diameter measurement system is shown in Fig. 2. The fiber holder for 500 mm gauge moves in 1 mm steps through the LSM measurement probe to send the diameter data to a PC, with an error level within ±0.1 μm. Figure 3 shows an example of the measurements. Uniform diameter sections, defined as a diameter variability within 1%, are indicated at the point 'A' in Fig. 3: these have been sampled for the tensile tests. Thus, for example, a sample defined as '10.0 μm' has diameter with lower and upper bounds of 9.9 μm and 10.1 μm, respectively.

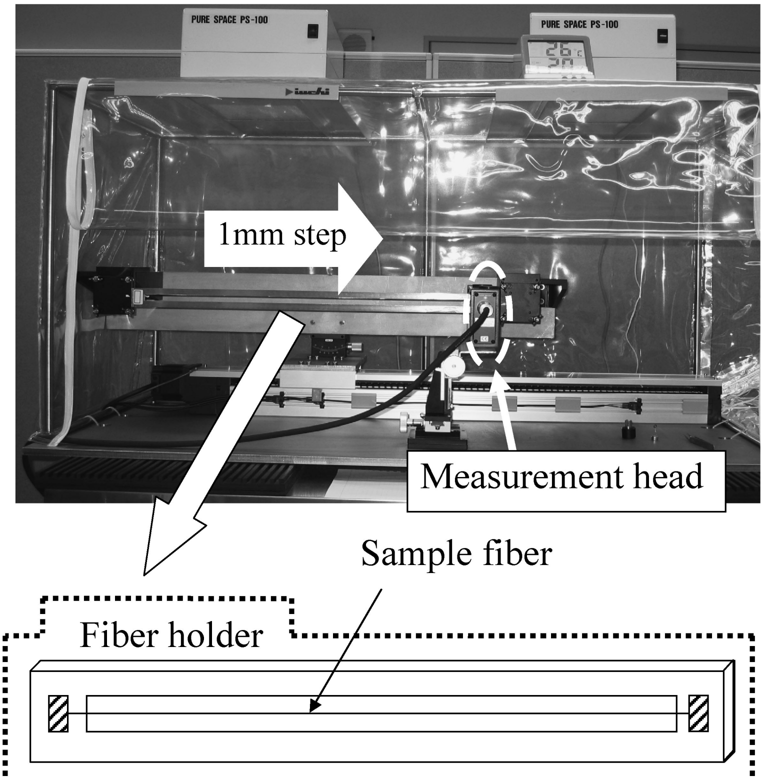

Figure 2. LSM measurement system.

2.2. Single fiber tensile test

An Instron universal tensile test system model 5542 with 10 N load cell was set at a crosshead speed of 0.1 mm/min for the single fiber tensile tests. Uniform diameter sections of Tyranno ZMI fiber have been prepared as depicted in Fig. 4 as the test sample. A paper tab was prepared with a central slot of 30 mm length. Then a portion, which had been confirmed to be of uniform diameter, was glued onto the tab with a elastic glue (Cilex clear, Konishi Co.) to minimize a stress concentration at the glued sections. In addition, samples fractured within 5 mm of each end were excluded from the statistical analyses data in order to avoid any bias by the clamp and glue. Thus, the central 20 mm was redefined as the gauge length out of the 30 mm sample fibers. The samples were immersed in an alpha-olefin sulfonate (AOS)-based surfactant during the tensile tests to recover the fragments and assess if the fracture sections were within the 20 mm gauge.

2.3. Data analysis

The data of 60 single fiber tensile tests were divided on the parameter search through the Weibull plot into two expedient groups as 'large diameter' group (the data from

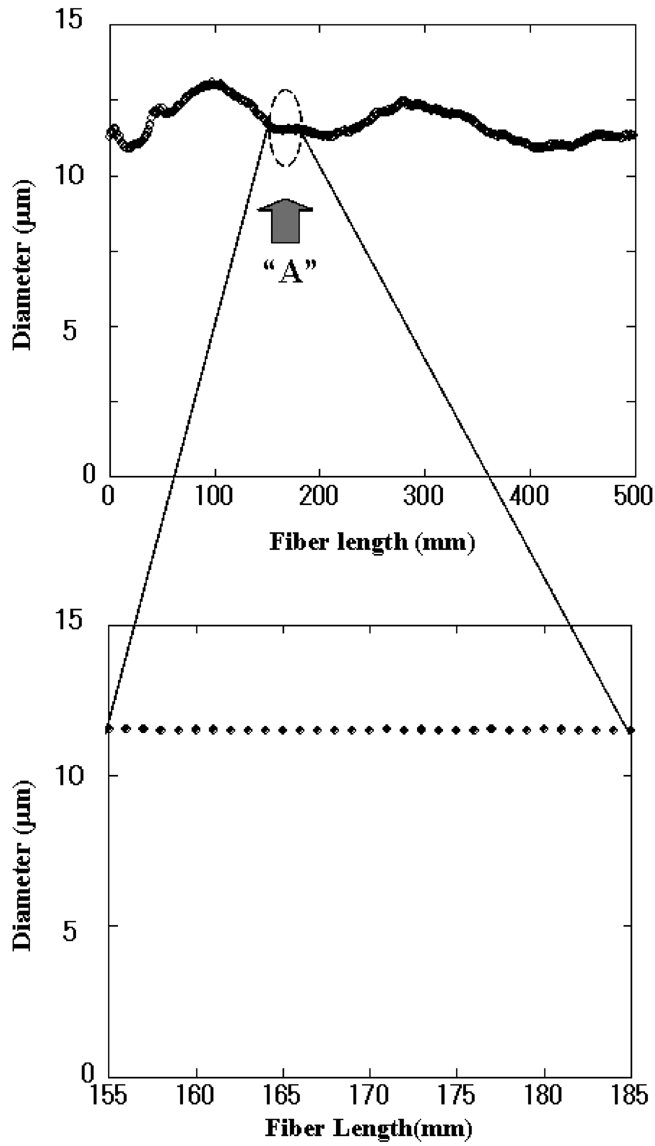

Figure 3. A result of LSM measurement.

the largest diameter sample to the 30th), and 'small diameter' group (the data from the 31st largest diameter sample to the 60th).

The two groups were expected to provide consistent sets of shape and scale parameters if the Weibull model reproduced the size effect. However, a percentage of 'large diameter' portions of amorphous Tyranno ZMI fiber may be locally crystallized in the precursor cure and pyrolysis process to negatively bias the strength from the Weibull scaling. In addition, alignment disorder could lead to more aggressive bending load in large diameter portion than in the more flexible

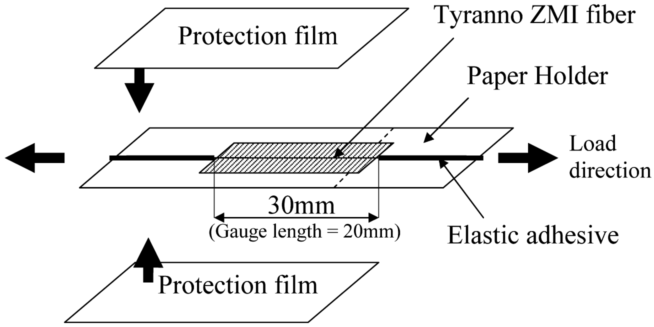

Figure 4. Single fiber tensile test specimen.

small diameter portion. The effect of these properties on Weibull shape and scale parameters was not negligible, such that the values were found to be inconsistent between the two groups.

2.4. SEM fractography

We believed that the fracture surface might reveal some exceptional factors that negate the strength size effect scaling of the Weibull model. Thereby each fracture surface of Tyranno ZMI sample was analyzed using a scanning electron microscope S-4700 (Hitachi Co.) to detect the fracture origin at the center of river pattern, to classify the characteristics, and to assess if fiber diameter affects the percentage of fracture dominant origins.

3. EXPERIMENTAL RESULTS

Figure 5 and Table 2 depict the 60 results of single fiber tensile test. A border of 11.5 μm in Fig. 5 was expediently set between two groups of 30 data sets designated as the 'large diameter group' and 'small diameter group'. The symbols A to F in Table 2 and Fig. 6 were defined on the fracture origin classifications as follows. Group A, which was found in 24 out of 60 samples, represents the samples without notable nucleation points, such as contaminant particles, voids and pre-cracks. Group B, which was found in 16 out of 60 samples, is for the samples with particles at the fiber side surface of fracture nucleation points. Group C, which was found in 9 out of 60 samples, is for the samples with embedded particles in the fiber volume. Group D, which was found in 4 out of 60 samples, is for the samples with pre-cracks at the side section of fibers. Group E, which was found in 5 out of 60 samples, is for the samples with agglomerates at the fracture origins. Finally, Group F, which was found in 2 out of 60 samples, is for the samples with the fracture nucleation points inside the circumference of the cross-sections. The subscription $_{\mathrm{mir}}$ represents the samples with large mirror zone around 10% of the fracture surface area. Figure 6, D and E, shows the example as D_{mir} and E_{mir} The case of $_{\mathrm{mir}}$ was found in 7 out of 60 samples and only in D and E.

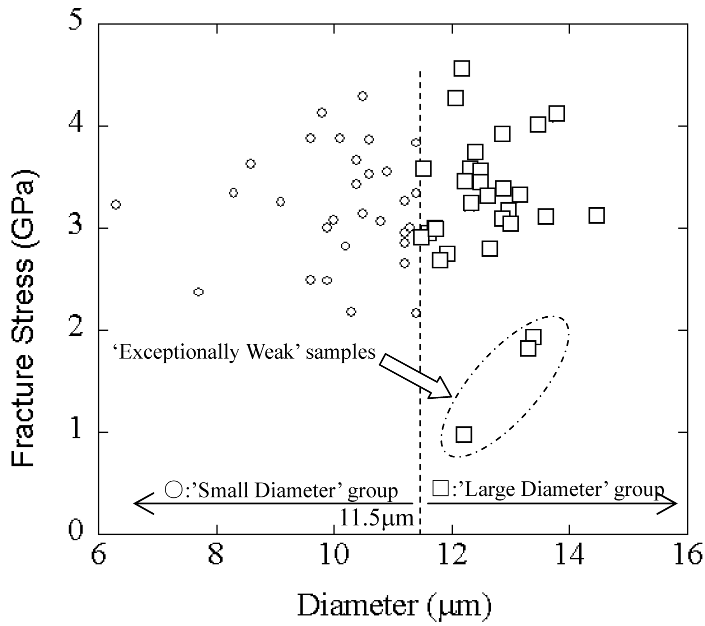

Figure 5. Single fiber tensile test results.

4. STATISTICAL ANALYSES AND DISCUSSIONS

Three 'exceptionally weak' samples were found in the 'large diameter group', as depicted in Fig. 5. The statistical bias of the data was assessed on Weibull strength scaling, applying a single-modal Weibull model.

4.1. Weibull analyses

The single-modal Weibull model and its modifications have often been applied for the strength size effect scaling of brittle materials [4–7]. In this work, a Weibull distribution function $F(\sigma)$ has been defined as follows.

$$F(\sigma) = 1 - \exp\left[-\frac{D}{D_0}\left(\frac{\sigma}{\sigma_0}\right)^m\right], \tag{1}$$

where m is a shape parameter, σ_0 is a scale parameter, D is the fiber diameter, and D_0 is a standard diameter defined as 10.2 μm, which has been expediently set with the mean value of 'small diameter' sample group. SEM fractography revealed that the fracture origins were localized in the region close to the fiber surface. Thus, the relation

$$S/S_0 = (\pi Dl/\pi D_0 l) = D/D_0$$

may be suitable as the size effect term, where S is the fiber side section area and l is the gauge length. When the fracture origins were uniformly distributed over

Table 2.
Single fiber tensile test results

'Small diameter' group			'Large diameter' group		
Diameter (μm)	Strength (GPa)	Defect class	Diameter (μm)	Strength (GPa)	Defect class
6.3	3.22	*B*	11.5	2.90	*C*
7.7	2.37	D_{mir}	11.5	3.57	*A*
8.3	3.34	*B*	11.6	2.94	*A*
8.6	3.63	*A*	11.7	2.98	*F*
9.1	3.25	*B*	11.7	2.99	*A*
9.6	3.88	*B*	11.8	2.66	*B*
9.6	2.49	*C*	11.9	2.71	*B*
9.8	4.12	*B*	12.1	4.27	*A*
9.9	2.48	E_{mir}	12.2	0.94	E_{mir}
9.9	3.00	*D*	12.2	3.43	*A*
10.0	3.07	*A*	12.2	4.55	*A*
10.1	3.87	*B*	12.3	3.55	*C*
10.2	2.82	*A*	12.3	3.21	*A*
10.3	2.17	E_{mir}	12.4	3.74	*A*
10.4	3.66	*A*	12.5	3.43	*A*
10.4	3.42	*A*	12.5	3.51	*A*
10.5	4.29	*A*	12.6	3.30	*B*
10.5	3.13	*A*	12.7	2.77	*C*
10.6	3.53	*B*	12.9	3.91	*A*
10.6	3.86	*C*	12.9	3.07	*C*
10.8	3.06	*C*	12.9	3.38	*B*
10.9	3.55	*C*	13.0	3.02	*A*
11.2	2.95	*A*	13.0	3.17	*C*
11.2	3.26	*B*	13.2	3.30	*A*
11.2	2.65	*B*	13.3	1.80	D_{mir}
11.2	2.85	*B*	13.4	1.92	E_{mir}
11.3	3.00	*A*	13.5	4.00	*F*
11.4	3.83	*A*	13.6	3.10	*D*
11.4	2.16	E_{mir}	13.8	4.09	*A*
11.4	3.34	*B*	14.5	3.10	*B*

the fracture surface, and thus uniformly throughout the volume V, the term D/D_0 should be replaced by $(D/D_0)^2$ as $V = (\pi/4) \cdot D^2 l$.

4.2. A bias on Weibull scaling

The shape parameter m and the scale parameter σ_0 have been derived through the Weibull plot on the relationship as follows.

$$\ln \ln\left(\frac{1}{1 - F(\sigma)}\right) - \ln\left(\frac{D}{D_0}\right) = m \ln \sigma - m \ln \sigma_0. \tag{2}$$

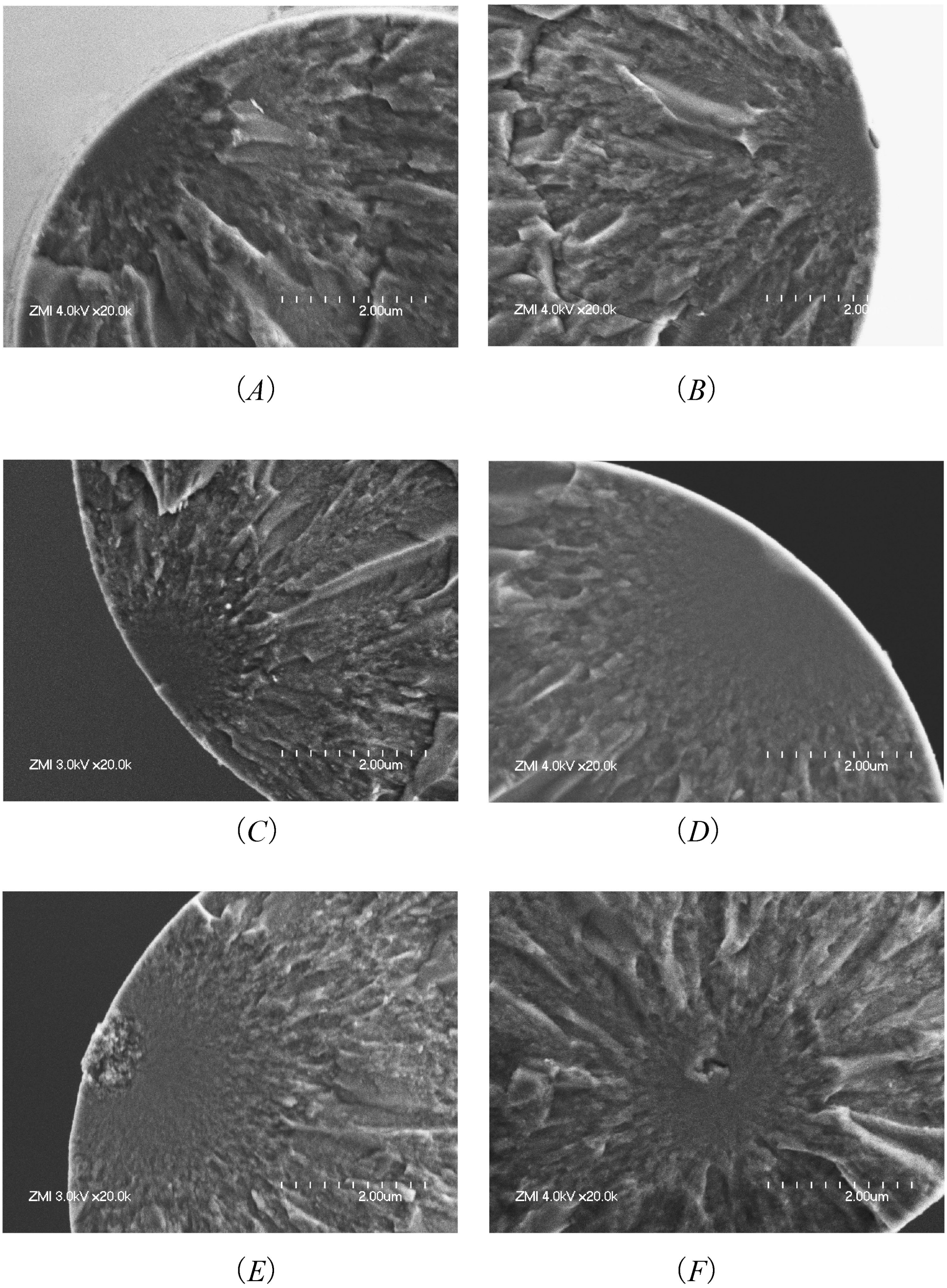

Figure 6. SEM micrographs of defect class A to F (examples) (A), (B), (C), (D), (E), (F).

The accumulated probability of fracture $F(\sigma)$ was approximated with a median rank method as follows.

$$F_i = \frac{i - 0.3}{n + 0.4}, \tag{3}$$

where n is the sample number and i is the rank of a sample in ordering the test results from the lowest stress to rupture to the highest.

The following results have been derived by applying the relationship (1) to (3) to the test results. Figure 7 depicts the Weibull plot, which implies that limited number of extremely weak samples bias the slope, thus, the derived parameters. The 'large diameter' and 'small diameter' 30 data set groups in Table 2 have provided the two

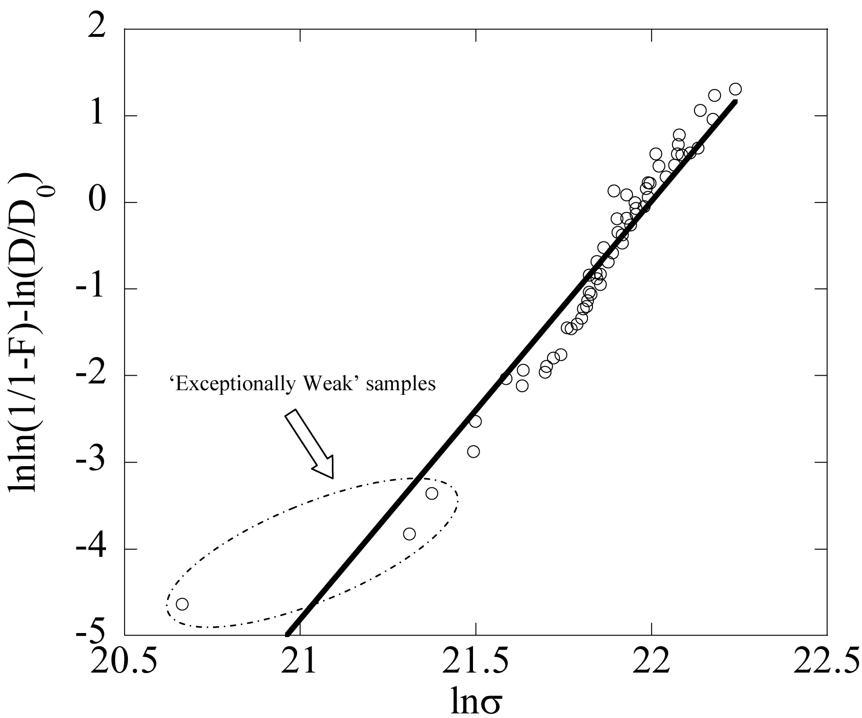

m	σ_0 (Pa)	Mean (Pa)	Variance	Standard deviation (Pa)
4.83	3.49×10^9	3.19×10^9	4.16×10^{17}	6.45×10^8

Figure 7. Weibull plot (all samples).

Weibull plots in Fig. 8 of the distribution functions as follows.

$$\text{‘Small diameter’ group:} \quad F(\sigma) = 1 - \exp\left[-\frac{D}{10.2}\left(\frac{\sigma}{3.44 \times 10^9}\right)^{6.51}\right]. \tag{4}$$

$$\text{‘Large diameter’ group:} \quad F(\sigma) = 1 - \exp\left[-\frac{D}{10.2}\left(\frac{\sigma}{3.77 \times 10^9}\right)^{3.73}\right]. \tag{5}$$

It was found that the shape parameter m was smaller in the ‘large diameter’ samples; thus the variance of fracture stress is larger than those of ‘small diameter’ samples. Thereby the Weibull shape parameter has been found dependent on fiber diameter.

4.3. An estimated Weibull distribution of ‘ideal’ Tyranno ZMI fiber strength

The two plots in Fig. 8 can be shown to be almost identical if a limited percentage of weak samples are excluded from the Weibull scaling. Thereby, an imaginary

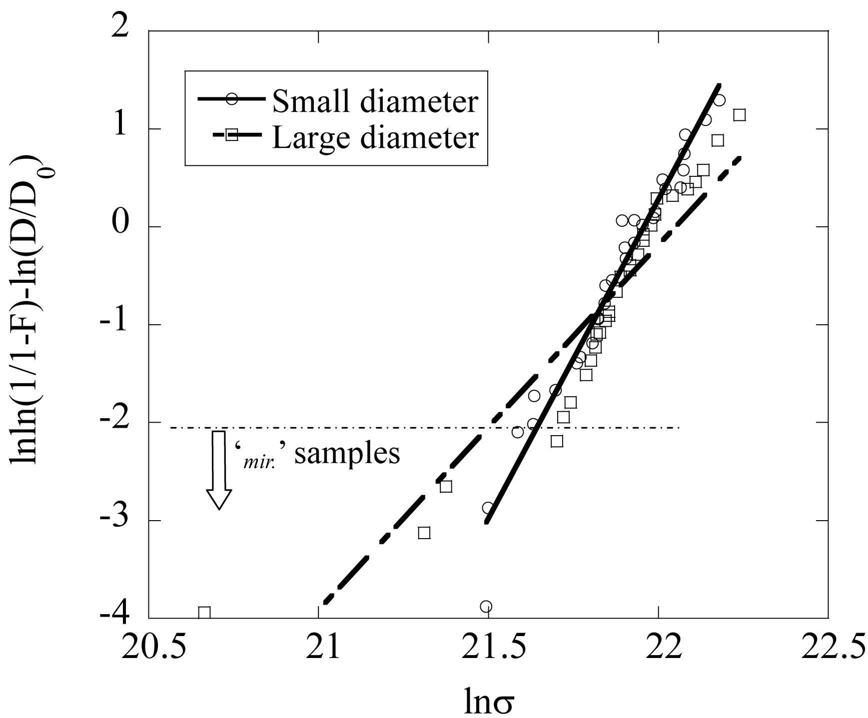

Diameter	m	σ_0 (Pa)	Mean (Pa)	Variance	Standard deviation (Pa)
Small diameter	6.51	3.44×10^9	3.21×10^9	3.14×10^{17}	5.60×10^8
Large diameter	3.73	3.77×10^9	3.18×10^9	5.32×10^{17}	7.29×10^8

Figure 8. Weibull plots (divided into two groups).

'ideal' Tyranno ZMI fiber strength is created here by excluding some of the data in the Weibull scaling.

The samples of large mirror zone, or the $_{\rm mir}$ in Table 2, were excluded in the scaling as they were localized in the weakest strength side. As is seen in Table 2, the samples with $_{\rm mir}$ were found only in *D* or *E* and the probabilities of existence were almost identical between the 'large diameter' group and 'small diameter' group. However, the $_{\rm mir}$ samples in Fig. 8 showed clearly a smaller strength in the 'large diameter' group than in the 'small diameter' group. This implies that the factor of $_{\rm mir}$ can have a greater negative effect on the strength in the 'large diameter' portion than in the 'small diameter' portion.

Figure 9 shows the Weibull scaling of the sample numbers 26 in 'small diameter' group and 27 in 'large diameter' group after excluding the data of $_{\rm mir}$. The derived

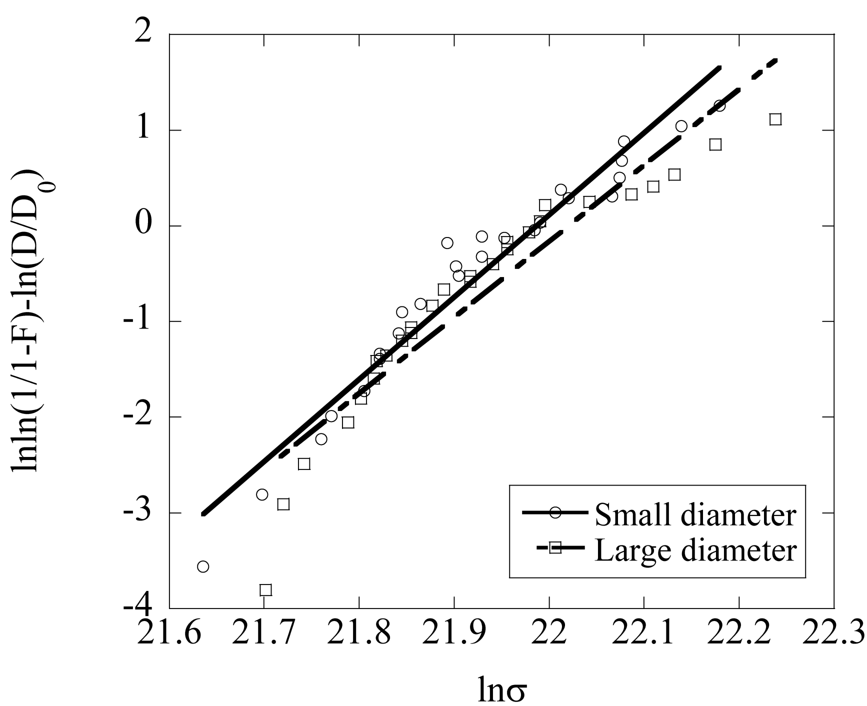

Diameter	m	σ_0 (Pa)	Mean (Pa)	Variance	Standard deviation (Pa)
Small diameter	8.59	3.54×10^9	3.35×10^9	2.07×10^{17}	4.55×10^8
Large diameter	7.95	3.66×10^9	3.36×10^9	2.34×10^{17}	4.83×10^8

Figure 9. Weibull plots ($_{\rm mir}$ samples: removed).

Weibull distribution functions were as follows.

$$\text{'Small diameter' group:} \quad F(\sigma) = 1 - \exp\left[-\frac{D}{10.2}\left(\frac{\sigma}{3.54 \times 10^9}\right)^{8.59}\right]. \tag{6}$$

$$\text{'Large diameter' group:} \quad F(\sigma) = 1 - \exp\left[-\frac{D}{10.2}\left(\frac{\sigma}{3.66 \times 10^9}\right)^{7.95}\right]. \tag{7}$$

The two Weibull distribution functions were found almost identical by excluding the data of D_{mir} and E_{mir}, as is seen in Fig. 9 and the relationships of equations (6) and (7); thus, the shape parameter m and scale parameter σ_0 are found to be less variable with diameter. In addition, the mean strengths have been improved both in the 'small diameter' group from 3.21 GPa to 3.35 GPa and in the 'large diameter' group from 3.18 GPa to 3.36 GPa. It is also noted that the shape parameter m more drastically increased to 7.95 from 3.73 in the 'large diameter' group than to 8.95 from 6.51 in the 'small diameter' group. This implies that limitation in the fiber diameter up to 'small diameter' level may neutralize the bias by the $_{\text{mir}}$ effect on the strength, and hence lead to a drastic improvement in the small variance even without the investment for refinement of the precursor material.

5. CONCLUSION

An examination of a single-modal Weibull model has been focused on the effect on strength of the size of Tyranno ZMI fiber. SEM fractography has revealed a relationship of some particular fracture origins with the tensile strength degradation and the diameter dependence. The following conclusions have been reached from the experimental results and the Weibull scaling. With Tyranno ZMI Si-Zr-C-O fiber, the parameters of the single-modal Weibull model are dependent on the sample diameter. The shape parameter assumed a drastically smaller value on the samples with diameter over 11.5 μm than on the samples with diameter of less than 11.5 μm. Thus, the Weibull model is inadequate to reproduce the effect of diameter size on the strength. However, it implies that Tyranno ZMI fiber has the potential to considerably reduce the strength variance by controlling the diameter to values below 11.5 μm.

REFERENCES

1. E. E. Bloom, The challenge of developing structural materials for fusion power systems, *J. Nuclear Mater.* **258–263**, 7–17 (1998).
2. H. Kaya, The applications of ceramic-matrix composites to the automotive ceramic gas turbine, *Compos. Sci. Technol.* **59**, 861–872 (1999).
3. A. Hasegawa, A. Kohyama, R. H. Jones, L. L. Snead, B. Riccardi and P. Fenici, Critical issues and current status of SiC/SiC composites for fusion, *J. Nuclear Mater.* **283–287**, 128–137 (2000).
4. A.-A. F. Tavassoli, Present limits and improvements of structural materials for fusion reactors – a review, *J. Nuclear Mater.* **302**, 73–88 (2002).

5. R. H. Jones, L. Giancarli, A. Hasegawa, Y. Katoh, A. Kohyama, B. Riccardi, L. L. Snead and W. J. Weber, Promise and challenges of SiC_f/SiC composites for fusion energy applications, *J. Nuclear Mater.* **307–311**, 1057–1072 (2002).
6. W. Weibull, A statistical distribution function of wide applicability, *J. Appl. Mech.* **18**, 293–297 (1951).
7. S. van der Zwaag, The concept of filament strength and the Weibull Modulus, *J. Test. Eval.* **17**, 292–298 (1989).
8. D. M. Wilson, Statistical tensile strength of Nextel^{TM}610 and Nextel^{TM}720 fibres, *J. Mater. Sci.* **32**, 2535–2542 (1997).
9. M. R. Gurvich, A. T. Dibenedetto and A. Pegoretti, Evaluation of the statistical parameters of a Weibull distribution, *J. Mater. Sci.* **32**, 3711–3716 (1997).
10. V. Lavaste, J. Besson and A. R. Bunsell, Statistical analysis of strength distribution of alumina based single fibres accounting for fibre diameter variations, *J. Mater. Sci.* **30**, 2042–2048 (1995).
11. Y. T. Zhu, W. R. Blumenthal, S. T. Taylor and T. C. Lowe, Analysis of size dependence of ceramic fiber and whisker strength, *J. Amer. Ceram. Soc.* **80**, 1447–1452 (1997).
12. I. J. Davies and T. Ishikawa, Bundle to bundle variation of mean fiber radius for Tyranno LoxM Si-Ti-C-O fibers, *J. Mater. Sci. Lett.* **20**, 505–507 (2001).
13. Y. Zhang, X. Wang, N. Pan and R. Postle, Weibull analysis of the tensile behavior of fibers with geometrical irregularities, *J. Mater. Sci.* **37**, 1401–1406 (2002).
14. M. Shibuya, Tyranno fiber and Tyranno fiber reinforced composites, *Fine Ceramics Report* **11**, 240–244 (1993) (in Japanese).
15. T. Morimoto, Statistics on the strength of ceramic fiber bundle, *Internat. J. Mater. Prod. Technol.* **16**, 22–31 (2001).
16. T. Morimoto, S. Nakagawa and S. Ogihara, Bias in the Weibull strength estimation of a SiC fiber for the small gauge length case, *JSME Internat. J. Series A* **48**, 194–198 (2005).
17. K. Kumagawa, H. Yamaoka, M. Shibuya and T. Yamamura, Fabrication and mechanical properties of new improved Si-M-C-(O) Tyranno fiber, *Ceram. Engng Sci. Proc.* **19**, 65–72 (1998).